

# Preparation of mesoporous silica with poly(oxyethylene)/poly(oxybutylene)/poly(oxyethylene) triblock copolymers as templates

Yaser A. I. Abu-Lebdeh, Peter M. Budd\*<sup>a†</sup> and V. Mark Nace<sup>b</sup>

<sup>a</sup>Department of Chemistry, University of Manchester, Manchester, UK M13 9PL

<sup>b</sup>The Dow Chemical Company, Texas Operations, Research and Development, Freeport, Texas 77541, USA

The phase behaviour in neutral and acid aqueous solution is reported for two poly(oxyethylene)/poly(oxybutylene)/poly(oxyethylene) (EBE) triblock copolymers, of composition  $E_{33}B_{10}E_{33}$  and  $E_{43}B_{14}E_{43}$ . Micellar solutions of both copolymers were utilised for templated-silica synthesis under acidic conditions. Calcination of the silica products gave mesoporous materials. The  $E_{33}B_{10}E_{33}$ -templated silica exhibited a spherical morphology, whilst the  $E_{43}B_{14}E_{43}$ -templated silica comprised irregularly shaped particles.

## Introduction

Mesoporous materials, with pore diameters in the range 2–10 nm, have recently attracted much attention for potential application in catalysis and separation processes. In 1992, Mobil researchers reported the surfactant-directed synthesis of a family of mesostructured silicas (denoted M41S).<sup>1</sup> Cationic surfactants were utilised and hexagonal (MCM-41), cubic (MCM-48) and lamellar (MCM-50) phases were obtained. Removal of surfactant by calcination yielded mesoporous inorganic solids. The pore size of the product could be controlled by varying the chain length of the surfactant used and by the addition of organic auxiliaries to the synthesis mixture.

This approach has been extended through the use of different types of surfactant and to the formation of a variety of metal oxide structures. Pinnavaia and co-workers have investigated the use of neutral primary amine surfactants<sup>2</sup> and non-ionic surfactants incorporating oxyethylene sequences, including a poly(oxyethylene)/poly(oxypropylene)/poly(oxyethylene) (EPE) triblock copolymer (Pluronic 64L).<sup>3,4</sup> Zhao *et al* have recently reported the synthesis of well ordered mesoporous silica (denoted SBA-15) utilising EPE copolymers.<sup>5</sup> Most syntheses are carried out at moderate surfactant concentrations and the mesostructured materials are obtained as precipitates. Göltner, Attard and colleagues, using high concentrations of nonionic surfactants<sup>6,7</sup> and polystyrene/poly(oxyethylene) block copolymers<sup>8</sup> have formed monoliths with mesostructures that directly reflect those of initial liquid crystalline phases.

The present contribution concerns the use of poly(oxyethylene)/poly(oxybutylene)/poly(oxyethylene) (EBE) triblock copolymers in the preparation of mesostructured precipitates. Tetraethoxysilane (TEOS) is utilised as the silica precursor and the synthesis is carried out at moderate polymer concentrations under acid conditions.

Copolymers of ethylene oxide and 1,2-butylene oxide have been studied academically for some years<sup>9–19</sup> and were commercialised by Dow in 1993.<sup>20–22</sup> Two commercial copolymers were used in this study. Since their phase behaviour has not previously been reported, and the effect of the acid conditions used in the silica synthesis is unknown, their phase diagrams were investigated, both in neutral aqueous solution and in the presence of acid, as part of the present work.

## Experimental

### Copolymers

Two EBE triblock copolymers from Dow Chemical Company were used in this work: B20-3800 (Batch No. GI04016105) and B20-5000 (Batch No. GE01016102). A study of the molecular characteristics and micellization behaviour of these samples has been published.<sup>21</sup> Both polymers are specified as containing 79 wt.% oxyethylene, and number-average molar masses,  $\bar{M}_n$ , are given as 3660 g mol<sup>-1</sup> for B20-3800 and 4790 g mol<sup>-1</sup> for B20-5000, suggesting the formulae are  $E_{33}B_{10}E_{33}$  and  $E_{43}B_{14}E_{43}$ , respectively (E = oxyethylene unit, B = oxybutylene unit). Characterization of these samples in Manchester gave results only slightly different from the specified values.<sup>21</sup> Both samples contain 2–3 mol% homopoly(oxyethylene). The sample of B20-3800 was shown by <sup>13</sup>C NMR to contain about 5 mol% B ends. The E-block-length distribution in EBE copolymers prepared by anionic polymerization is quite broad, and non-ethoxylated B-block ends may arise, because of the relatively slow initiation of the E blocks by the secondary oxyanion of the B end. However, the gel permeation chromatography (GPC) curves of the EBE block copolymers show a single narrow peak, unlike those for commercial EPE copolymers which typically feature two peaks or a peak with a shoulder.

### Phase diagrams for EBE block copolymers

Solutions of copolymer at various concentrations in the range 1–80 wt.% were prepared in water, 1 M aqueous HCl and 4 M aqueous HCl. Polymer and solvent (total weight 2 g) were weighed into a small sample tube. The tube was heated to 90 °C to obtain a homogeneous system, then cooled and allowed to stand for two days at 5 °C or less. Transitions between mobile fluid and immobile gel phases were investigated by a tube-inversion method. Tubes containing solution were observed whilst being slowly heated (0.5 °C min<sup>-1</sup>) within the range 0–90 °C, in a water bath. The tubes were inverted after every minute. When checked, gel phases were found to be immobile in the inverted tube over a period of weeks.

Solutions were also investigated by polarising microscopy, using a Nikon Optishot polarizing microscope equipped with a Mettler FP82HT hot stage temperature controller. Samples were placed on glass slides and covered with thin cover slips to reduce evaporation of water. Observations were at  $\times 100$

†E-mail: Peter.Budd@man.ac.uk

magnification and a heating rate of  $1\text{ }^{\circ}\text{C min}^{-1}$  was used over the range  $0\text{--}80\text{ }^{\circ}\text{C}$ .

### Preparation of mesoporous silica

In preliminary studies, the copolymer concentration, pH and ratio of acid: $\text{H}_2\text{O}$ :surfactant were optimised to give the maximum intensity of the X-ray diffraction peak for the product. A typical preparation is described below. The silica syntheses reported here were carried out at copolymer concentrations of 12 wt.% for  $\text{E}_{35}\text{B}_{10}\text{E}_{35}$  and 10 wt.% for  $\text{E}_{43}\text{B}_{14}\text{E}_{43}$ .

Copolymer (2.4 g  $\text{E}_{33}\text{B}_{10}\text{E}_{33}$  or 2.0 g  $\text{E}_{43}\text{B}_{14}\text{E}_{43}$ ) was dissolved in 17.6 g water and concentrated HCl added to adjust the pH to 1. The acidified solution was stirred for 30 min to solubilize the copolymer, then TEOS (2.78 g for  $\text{E}_{33}\text{B}_{10}\text{E}_{33}$  or 2.317 g for  $\text{E}_{43}\text{B}_{14}\text{E}_{43}$ ) added dropwise with vigorous stirring. The mixture was stirred for 3 h and then placed in an oven at  $60\text{ }^{\circ}\text{C}$  overnight. After cooling to room temperature, the solid product was recovered by filtration on a Buchner funnel, washed with distilled water and allowed to dry.

Calcination was carried out in air at  $220\text{ }^{\circ}\text{C}$  for 2 h, then at  $540\text{ }^{\circ}\text{C}$  for 6 h. The heating rate was  $1\text{ }^{\circ}\text{C min}^{-1}$ .

### Characterization of silica products

Powder X-ray diffraction (XRD) patterns were obtained using a Philips PW 1730 generator (Cu- $\text{K}\alpha$  radiation,  $\lambda = 0.154$  nm) and a Philips PW 1050 diffractometer. Samples for analysis were dispersed in ethanol and a few drops of the dispersion placed uniformly on a glass slide.

Scanning electron microscopy (SEM) was performed on a JEOL 6200 scanning electron microscope.

Combined thermogravimetric analysis and differential thermal analysis (TG-DTA) was carried out on a Seiko SSC/5200 TG/DTA 220 instrument.

$\text{N}_2$  adsorption-desorption isotherms for calcined products were determined by a continuous flow method.<sup>23</sup>

## Results and Discussion

### Phase diagrams for EBE block copolymers

Phase diagrams for  $\text{E}_{33}\text{B}_{10}\text{E}_{33}$  in neutral and acidic aqueous solution are shown in Fig. 1. At concentrations above 65 wt.%, a transformation from immobile gel to mobile fluid is observed on raising the temperature. In the range 65–73 wt.%, the gel phase is isotropic, so is presumably cubic. At higher concentrations it exhibits birefringence, with an optical texture typical of a hexagonal phase. It can be seen in Fig. 1 that 1 M HCl has little effect on the phase diagram of  $\text{E}_{33}\text{B}_{10}\text{E}_{33}$ , but that

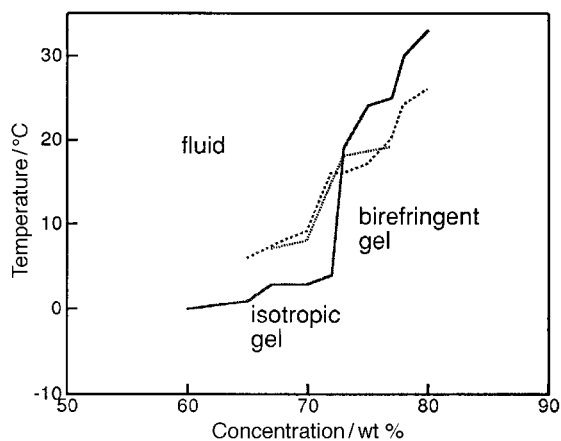


Fig. 1 Phase diagram for  $\text{E}_{33}\text{B}_{10}\text{E}_{33}$  copolymer in (···) water, (---) 1 M aq. HCl and (—) 4 M aq. HCl

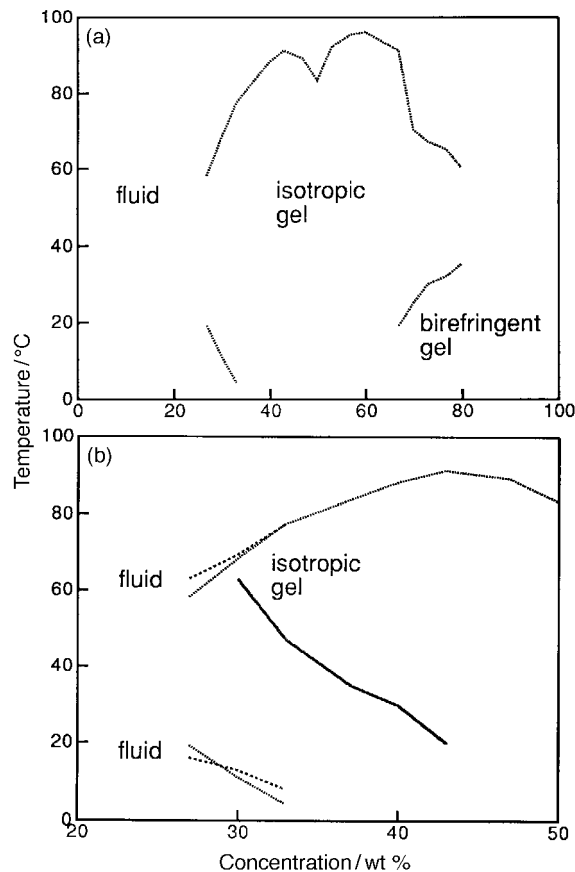


Fig. 2 Phase diagram for  $\text{E}_{43}\text{B}_{14}\text{E}_{43}$  copolymer (a) in water and (b) over the concentration range 20–50 wt.% in (···) water, (---) 1 M aq. HCl and (—) 4 M aq. HCl

4 M HCl has a more pronounced influence. Interestingly, 4 M HCl affects the cubic and hexagonal phases in opposite ways, lowering the temperature of the cubic→fluid transition, but raising the temperature of the hexagonal→fluid transition. Li,<sup>24</sup> using a wide range of techniques, has investigated the phase diagram in neutral aqueous solution for a polymer of composition  $\text{E}_{35}\text{B}_{10}\text{E}_{35}$  prepared in Manchester. Although the nominal composition is very similar to that of the Dow product studied here, the phase diagram differed in showing an extensive cubic region in the concentration range 40–60 wt.%. This illustrates the sensitivity of the phase behaviour to the distribution of block sizes as well as to overall composition.

Fig. 2(a) shows the phase diagram for  $\text{E}_{43}\text{B}_{14}\text{E}_{43}$  in neutral aqueous solution. At concentrations in the range 27–33 wt.%, a low temperature fluid→isotropic gel transition is seen as well as a high temperature gel→fluid transition. This has been observed previously by Ali.<sup>25</sup> At high concentrations there is evidence of a hexagonal phase. The effect of acid on the phase diagram is illustrated in Fig. 2(b). 1 M HCl has little effect, but in 4 M HCl the fluid→gel transition moves to higher temperatures.

### Characterization of silica products

X-Ray powder diffraction patterns are shown in Fig. 3 and 4 for  $\text{E}_{33}\text{B}_{10}\text{E}_{33}$ -templated and  $\text{E}_{43}\text{B}_{14}\text{E}_{43}$ -templated silica, respectively. Each product exhibits a peak at low angle, which increases in intensity and moves to slightly higher angles on calcination. Application of the Bragg equation to the peak maximum  $2\theta$  values gives the  $d$ -spacings listed in Table 1. Combined TG-DTA confirmed that copolymer was removed on calcination.

The morphology of  $\text{E}_{33}\text{B}_{10}\text{E}_{33}$ -templated silica is significantly different to that of  $\text{E}_{43}\text{B}_{14}\text{E}_{43}$ -templated silica. Fig. 5

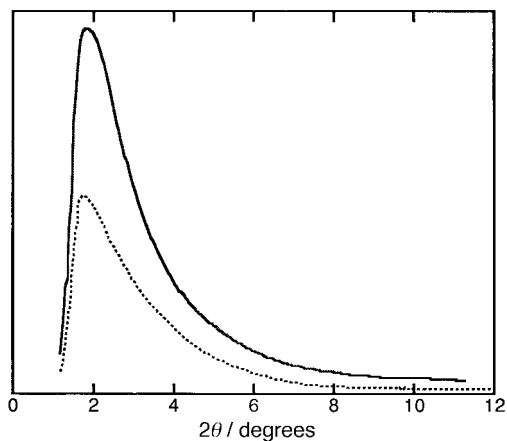


Fig. 3 Smoothed powder X-ray diffraction data for as-synthesised (---) and calcined (—)  $E_{33}B_{10}E_{33}$ -templated silica

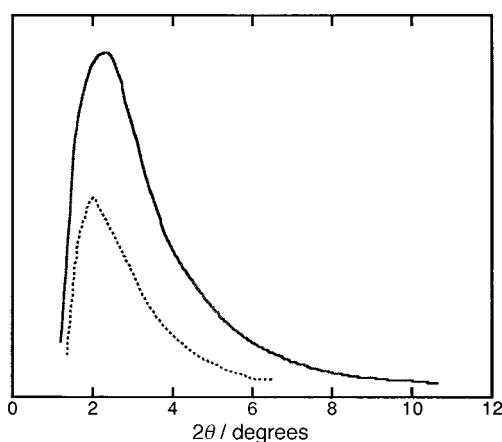


Fig. 4 Smoothed powder X-ray diffraction data for as-synthesised (---) and calcined (—)  $E_{43}B_{14}E_{43}$ -templated silica

Table 1 Bragg distances and specific surface areas for silica products

copolymer template	as-synthesised product $d/\text{nm}$	calcined product	
		$d/\text{nm}$	$A/\text{m}^2 \text{g}^{-1}$
$E_{33}B_{10}E_{33}$	5.0	4.8	505
$E_{43}B_{14}E_{43}$	4.3	3.8	520

shows scanning electron micrographs for  $E_{33}B_{10}E_{33}$ -templated silica, which comprises essentially spherical particles, with diameters in the region of 2.6  $\mu\text{m}$ . The  $E_{43}B_{14}E_{43}$ -templated silica (Fig. 6) consists of irregularly shaped particles.

$N_2$  adsorption-desorption isotherms are shown in Fig. 7 and 8 for calcined  $E_{33}B_{10}E_{33}$ -templated and  $E_{43}B_{14}E_{43}$ -templated silica, respectively. Both products give type IV isotherms, as commonly observed for mesoporous materials. The available data are insufficient for meaningful BET analysis or for a reliable determination of pore size distribution, but specific surface areas ( $A$ ) based on uptake at the beginning of the linear region (often referred to as point B)<sup>26</sup> are given in Table 1.

The results obtained here for EBE-templated silicas are comparable to those obtained by Bagshaw and Pinnavaia<sup>4</sup> for  $E_{13}P_{30}E_{13}$ -templated aluminas. There are insufficient data to assign conclusively a phase structure, but it may be similar to the hexagonal continuous structure described by Göltner *et al.*<sup>8</sup> Zhao *et al.*<sup>5</sup> have reported the use of EPE copolymers with larger blocks, such as  $E_{20}P_{70}E_{20}$ , which gave highly ordered silica with hexagonal symmetry.

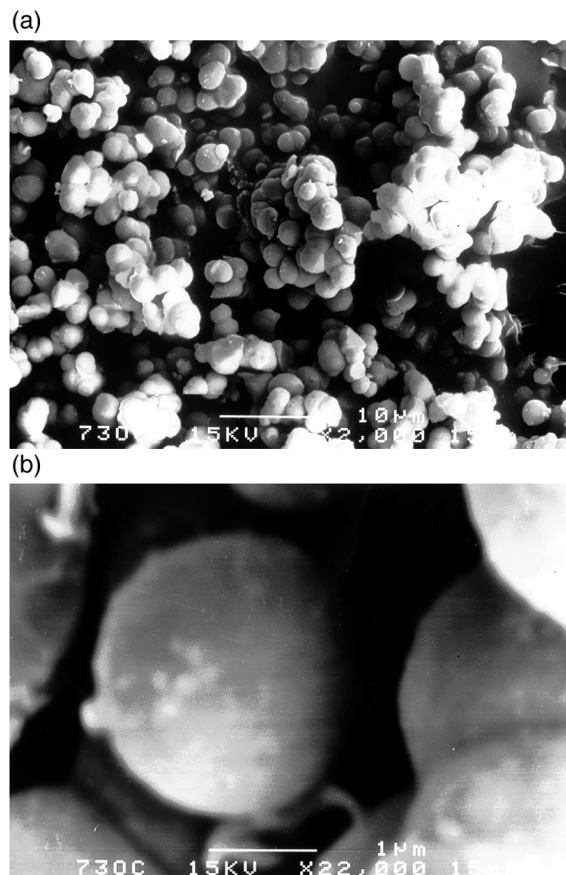


Fig. 5 Scanning electron micrographs of  $E_{33}B_{10}E_{33}$ -templated silica at (a) low magnification and (b) high magnification

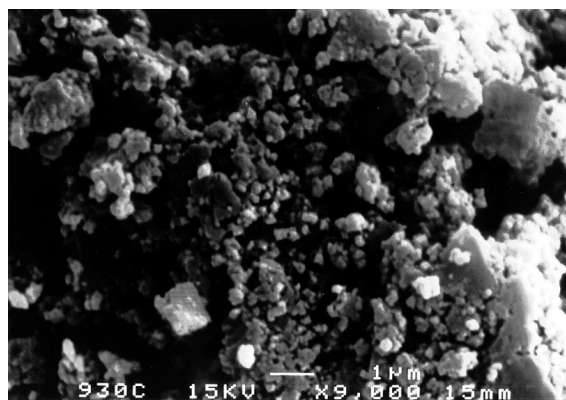


Fig. 6 Scanning electron micrograph of  $E_{43}B_{14}E_{43}$ -templated silica

#### Formation of mesostructured silica

At the concentrations employed in the silica syntheses (10–12 wt.%) the copolymers form isotropic micellar solutions, so a mesophase does not exist prior to addition of the silica precursor. Hydrolysis of TEOS and formation of oligomeric silicates is expected to occur rapidly at the low pH of these preparations, but a precipitate is not observed until after about 7 h of ageing at 60 °C. The formation of mesostructured silica may be considered to involve four processes:

- (1) Growth of oligomeric silicates.
- (2) Separation of a phase rich in organic copolymer and silicate oligomers. Driving forces for phase separation may involve (i) interactions between copolymer and silicate species and (ii) partial miscibility with solvent of growing silicate oligomer/copolymer complexes.
- (3) Microphase separation within the precipitate giving the mesostructure.

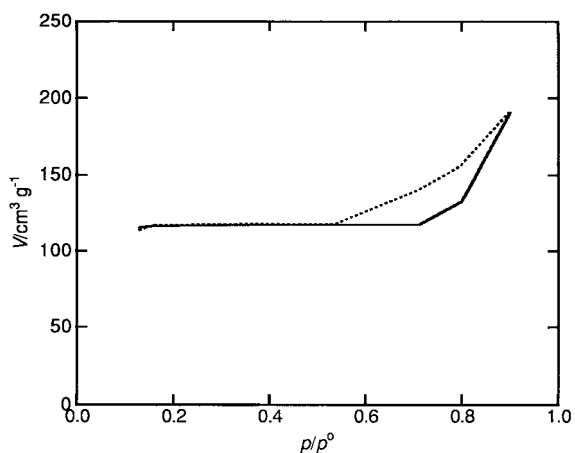


Fig. 7 N<sub>2</sub> adsorption (—) and desorption (----) isotherms for calcined E<sub>33</sub>B<sub>10</sub>E<sub>33</sub>-templated silica

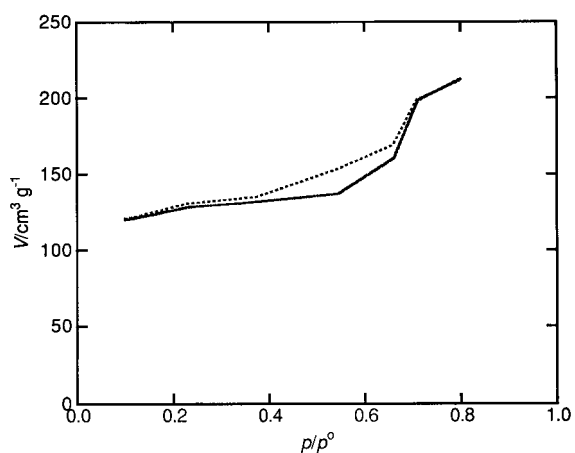


Fig. 8 N<sub>2</sub> adsorption (—) and desorption (----) isotherms for calcined E<sub>43</sub>B<sub>14</sub>E<sub>43</sub>-templated silica

(4) Further silicate polymerization and crosslinking to fix the mesostructure.

We are grateful to Dr B. Sakakini, UMIST, for assistance in obtaining N<sub>2</sub> adsorption-desorption isotherms

## References

- 1 J. S. Beck, J. C. Vartuli, W. J. Roth, M. E. Leonowicz, C. T. Kresge, K. D. Schmitt, C. T.-W. Chu, D. H. Olsen, E. W. Sheppard, S. B. McCullen, J. B. Higgins and J. L. Schlenker, *J. Am. Chem. Soc.*, 1992, **114**, 10834.
- 2 P. T. Tanev and T. J. Pinnavaia, *Chem. Mater.*, 1996, **8**, 2068.
- 3 S. A. Bagshaw, E. Prouzet and T. J. Pinnavaia, *Science*, 1995, **269**, 1242.
- 4 S. A. Bagshaw and T. J. Pinnavaia, *Angew. Chem., Int. Ed. Engl.*, 1996, **35**, 1102.
- 5 D. Zhao, J. Feng, Q. Huo, N. Melosh, G. H. Fredrickson, B. F. Chmelka and G. D. Stucky, *Science*, 1998, **279**, 548.
- 6 G. S. Attard, J. C. Glyde and C. G. Göltner, *Nature*, 1995, **378**, 366.
- 7 C. G. Göltner and M. Antonietti, *Adv. Mater.*, 1997, **9**, 431.
- 8 C. G. Göltner, S. Henke, M. C. Weissenberger and M. Antonietti, *Angew. Chem., Int. Ed. Engl.*, 1998, **37**, 613.
- 9 J. Myszkowski, J. Szymanowski, W. Goc and K. Alejski, *Tenside Deterg.*, 1982, **19**, 7.
- 10 J. H. Lee, J. Kopecek and J. Andrade, *Polym. Mater. Sci. Eng.*, 1987, **57**, 613.
- 11 W.-B. Sun, J.-F. Ding, R. H. Mobbs, F. Heatley, D. Attwood and C. Booth, *Colloid Surf.*, 1991, **54**, 103.
- 12 Y.-Z. Luo, C. V. Nicholas, D. Attwood, J. H. Collett, C. Price and C. Booth, *Colloid Polym. Sci.*, 1992, **270**, 1094.
- 13 C. V. Nicholas, Y.-Z. Luo, N.-J. Deng, D. Attwood, J. H. Collett, C. Price and C. Booth, *Polymer*, 1993, **34**, 138.
- 14 A. D. Bedells, R. M. Arafeh, Z. Yang, D. Attwood, F. Heatley, J. C. Padget, C. Price and C. Booth, *J. Chem. Soc., Faraday Trans.*, 1993, **89**, 1235.
- 15 Z. Yang, S. Pickard, N.-J. Deng, R. J. Barlow, D. Attwood and C. Booth, *Macromolecules*, 1994, **27**, 2371.
- 16 Y.-W. Yang, N.-J. Deng, G.-E. Yu, Z.-K. Zhou, D. Attwood and C. Booth, *Langmuir*, 1995, **11**, 4703.
- 17 Y.-W. Yang, Z. Yang, Z.-K. Zhou, D. Attwood and C. Booth, *Macromolecules*, 1996, **29**, 670.
- 18 Y.-W. Yang, Z. Ali-Adib, N. B. McKeown, A. J. Ryan, D. Attwood and C. Booth, *Langmuir*, 1997, **13**, 1860.
- 19 A. Kellarakis, V. Havredaki, G.-E. Yu, L. Derici and C. Booth, *Macromolecules*, 1998, **31**, 944.
- 20 V. M. Nace, R. H. Whitmarsh and M. W. Edens, *J. Am. Oil Chem. Soc.*, 1994, **71**, 777.
- 21 G.-E. Yu, Y.-W. Yang, Z. Yang, D. Attwood, C. Booth and V. M. Nace, *Langmuir*, 1996, **12**, 3404.
- 22 V. M. Nace, *J. Am. Oil Chem. Soc.*, 1996, **73**, 1.
- 23 F. M. Nelsen and F. T. Eggertsen, *Anal. Chem.*, 1958, **30**, 1387.
- 24 H. Li, PhD Thesis, University of Manchester, 1997.
- 25 M. Ali, MSc Dissertation, University of Manchester, 1996.
- 26 S. J. Gregg and K. S. W. Sing, *Adsorption, Surface Area and Porosity*, Academic Press, London, 2nd edn., 1982.

Paper 8/02354I; Received 26th March, 1998